

Effect Of Zinc Oxide Nanoparticles On Activity Of Cell Line (B16) Causes Skin Cancer

Basem Mohamed Abdul Latif^{1, a} , Mohanad W. Mahdi Alzubaidy^{1, b}

Department of Biology, College of Education for Pure Sciences, University of Diyala, Iraq

Abstract

The investigation and discovery of effective drugs for skin cancer has become an important target due to the widespread and dangerous spread of skin cancer throughout the world, so it is necessary to study this disease and discover the nanomaterials affecting it to reach effective treatments in order to eliminate this disease. In this study, zinc oxide nanoparticles (ZnO-NPs) were prepared by chemical lysis and sol-gel method, X-ray diffraction and scanning electron microscope (SEM) were used, in addition to the study of cytotoxicity. Assays of the toxic effect of ZnO-NPs at different concentrations (6.25-100 µg/ml) on melanoma cells using the (B16) mouse melanoma cell line, and the ex vivo Rat embryonic fibroblast (Ref) cell line. And by studying the ability of ZnO-NPs to inhibit the proliferation of cancer cells, the results of this study showed that there is an inhibitory activity for the growth of these cancer cells with statistical significance (highly significant). This gives hope for a successful treatment to eliminate skin cancer using nanoparticles as a material Unconventional used in the treatment of cancer.

Keywords: Nanoparticles, Cell line (B16), Skin Cancer, Cytotoxicity Assays

Introduction

Cancer is the second leading cause of death worldwide and the incidence of cancer is expected to increase in the future adding to the stress of limited healthcare resources which requires appropriate allocation of resources, cancer prevention, early diagnosis and curative cancer care [1]. Among the cancers that affect humans is skin cancer and non-melanoma skin cancer (NMSC), which is the most common type in the white population and both tumor entities show an increased incidence worldwide [2]. The use of nanotechnology in the pharmaceutical industry is a promising field as it uses nanomaterials (10-100 nm) that can take advantage of the unusual properties of nanomaterials such as high specific surface area and transferable shape and size, [3]. Wide types of nanoparticles with exciting properties are being synthesized and used in a wide range of biological applications [4]. The poor pharmacological properties of conventional anticancer drugs due to poor solubility, stability and metabolism pose different challenges in their cytotoxic efficacy, inefficiency and limited bio distribution. Therefore, it is necessary to develop effective formulations that can address the challenges and provide selective targeting of tumor sites without significant damage to healthy tissues [5].

Zinc oxide nanoparticles ZnO-NPs have an effective effect in eliminating skin cancer, which has become a major concern all over the world due to the high death rate due to this disease [6]. This study aimed to prepare and chemically characterize ZnO-NPs nanoparticles by liquid gel method, then investigate the effect of ZnO-NPs nanoparticles on the B16 cell line in terms of cytotoxicity.

Materials and working methods

The study was carried out by following several steps as shown below

Preparation of ZnO-NPs by sol-gel method as reported in [7]. Zinc acetate dissolved 0.1 M water in 100 mm non-ionic water on a magnetic rotor 450 cycles and at room temperature. Dissolve 0.1 M citric acid in 100 mm non-ionic water. The two solutions were mixed with continuous stirring with a magnetic rotating device, and the combined solution consisting of aqueous zinc acetate and citric acid was measured using the pH function of the device until it reached pH 7 by placing drops of ammonia. The mixture is then left on the magnetic rotor at a temperature of 80 °C and rotated at a speed of 450 revolutions until a white gelatinous liquid is formed. The resulting gel was placed on an hour bottle in an autoclave at 80 °C for 2 hours to produce a white powder. Finally, we put the white powder by the vine into the ceramic electric furnace to burn at 450 °C for 2½ hours, and for the purpose of finally producing calcination the white matter particles of ZnO-NPs nanoparticles are nailed.

FTIR spectrophotometry

Within the 4000-400 infrared spectrum of ZnO-NPs were measured using a Japanese-made infrared spectrophotometer, Shimadzu Corporation located in the Department of Chemistry Sciences/College of Education for Pure Sciences/University of Diyala, using the disc method [8] By taking a sample of 1 mg of ZnO-NPs and adding potassium bromide KBr-1 the components were mixed in a ceramic slurry and a transparent table was formed using the plunger and then placed in the above apparatus.

X-ray diffraction difference

X-ray diffraction (XRD) assays were performed at Kashan University/Iran using X-ray diffraction to determine their crystal structure, to describe crystalline materials and give information about the preferred structures, phases, crystal orientations (texture) and other structural parameters such as the average grain size calculated according to the formula Sharer [9] Crystallization and defects of crystals. X-ray diffraction is the imprint of periodic atomic arrangements in a given material [10].

Scanning Electron Microscopy (SEM)

The tests were carried out for ZnO-NPs nanoparticles recorded in a liquid gel manner to show the morphology and structure properties of the prepared in this way using the Scanner Electron Microscope at Kashan University / Liran device works on the imaging sample Power Zoom 25-250000 times and scans the sample at very high resolution as the beam interacts concentrated with the sample. By means of electrons colliding with atoms of the sample and transmitting signals that analyze the surface structure, the detectors convert the intensity of the electrons into a digital stored voltage and 3D images are formed that reach the size that it can measure from 1-5 nm [11]

Cytotoxicity Assays

Experiments were conducted on the cancer cell line (B16) taken from the mouse and the origin and description of this mentioned line [12]and comparing it with the normal line Rat embryonic fibroblast (Ref) until the cancer cells are transplanted, the following was done:

Cancer cell lines for vascular tissue culture 25 cm² containing RBMI-1640 medium were placed on 10% fetal calf serum, the container containing the cell suspension and culture medium was placed in a 5% incubator. carbon dioxide at a temperature of 37 °C for 24 hours, and after 24 hours of incubation, and to ensure that there is no contamination in cell culture and development, secondary cultures were made for them, and then the cells were examined using an inverted microscope to ensure that they were free of contamination and viability, were The cells

were then transferred to the growth chamber and the culture medium used was dried and the cells washed with phosphate-buffered saline (PBS). Phosphate saline was removed and repeated twice for 10 min each time a sufficient amount of trypsin/vericin was added into the cells and cells were placed for 30-60 s at 37°C and monitored until this occurred. Transformed from a single cell layer to single cells after being separated from the tissue culture vessel, the enzyme is then stopped by adding fresh culture medium containing 10% booster serum after distribution into new containers and then placed in a 5% CO₂ incubator at 37 °C for 24 h. The old culture medium was then dried and the contents of the 25poison2 tissue culture vessel treated with trypsin/viricin. Gently stir the flask to form a cell suspension, incubate in the incubator at 37 °C for 10 min, and then add 20 ml of culture medium to it. Containing serum and mixed well, and then assay was performed with MTT dye (3, 4, 5-dimethylthiazol-2-yl-2, 5-diphenyltetrazolium bromide [13]. The streak was seeded at 10,000 cells/pit using a plate Microliter for tissue culture.Distance 24 h. The addition of monolayers of cells ZnO-NPs at different concentrations (6.25-100. µg/ml) was confirmed for 24h. After of exposure time,culture medium was removed and cells were washed with phosphate-buffered salinethree times, after which 30 µM of dye at a MTT concentration of 2 mg/ml was added and culture plate was incubated at 37 °C for 3 h after which, 25 µL of the solution was added DMSO was inserted into each hole for 10 min and Platelayer was incubated again. The temperature of 37 °C was measured only by an ELISA device at 492 nm and then the cytotoxicity was calculated using the following equation: modified inhibition = A-B/A * 100

Where:

A is the optical density of the control (cells not treated with nanomaterial's)

B is the optical density of the samples (cells treated with nanomaterial's)

Cells (B16) and (Ref) as previously reported to study the morphological and volumetric changes of cells using IC50 semi-inhibited ZnO nanoparticles at a concentration of 27.36 and 2830 µg/ml respectively for 24 h after exposure time were stained with crystal. The dye was incubated with crystal violet at 37 h. for 10-15 minutes. The dye was gently washed off with tap water until the dye was completely removed. Cells were observed under an inverted microscope40X and take pictures with a digital camera attached to the microscope.

Results and Discussion

Infrared (FTIR) spectroscopy of ZnO-NPs.

The acquisition of ZnO-NPs by liquid gel method was confirmed by instantaneous infrared spectrometry where the wavelength of the beam appears (3306.04 cm⁻¹) and as shown in Figure (1), indicating the molecule's hydroxyl group attached to the molecule and the presence of an absorption band It has an area of (422.41 cm⁻¹) resulting from zinc nanoparticles. These results are consistent with the findings [11].

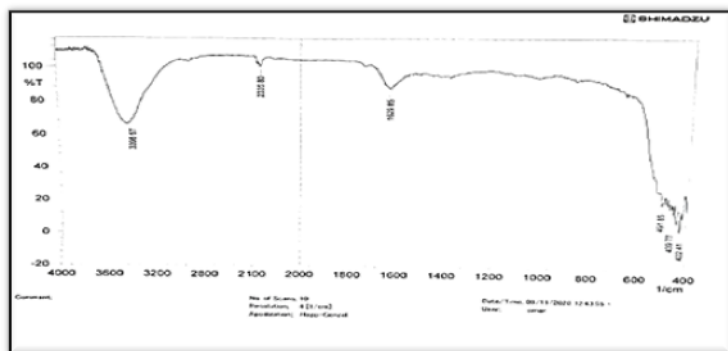


Figure 1 shows infrared (FTIR) spectra of ZnO-NPs. Nanoparticle

X-rays of ZnO-NPs.

Description of X-ray diffraction patterns of ZnO-NPs by analyzing these patterns, the locations of the peaks were known, where we observe the appearance of the levels [(101), (002), (101), (102), (110), (103), (200), (112), (201), (004), (202)] These vertices at the angles are: (68.0466, 66.4902, 62.8531, 56.6779, 47.6492, 36.3278, 34.4759, 31.8686, 72.5937 and 69.1559 and 77.0781 = θ) respectively, as shown in Figure (2). When comparing the orientation of these peaks and diffraction angles with the global numbered (36-1451) for ZnO-NPs nanoparticles as in Fig. It was found that it corresponds to a very large extent and agrees with the results of many studies [12].

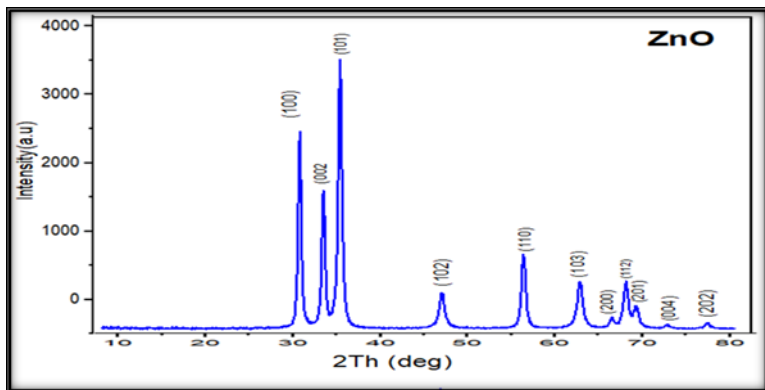


Figure 2 shows X-ray diffraction of ZnO-NPs nanoparticles. Explanation of peak levels

Scanning Electron Microscopy (SEM) of ZnO-NPs.

Figure 3 (SEM) images shows scanning electron microscopy of as-prepared ZnO-NP by liquid gel method, Magnification (50 KX). results of the analysis showed that most of the ZnO-NP are dense and spherical in shape, and it was found that the size of the prepared particles Approximately (37-62) nm, these results were more accurate in nanoscale shape and size with what has been achieved [16].

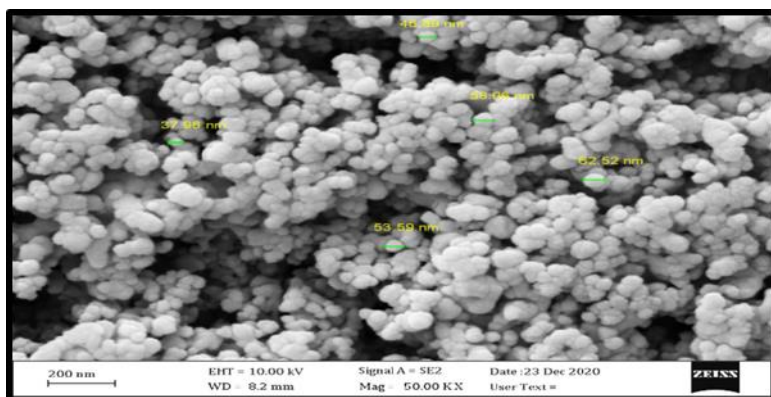


Figure 3 shows size measurements of ZnO-NPs by SEM (37-62) nm prepared by the sol-gel method.

Cytotoxicity assays.

Toxic effect of different concentrations of ZnO-NPs on (B16) cell growth as well, normal cell line (ref.) by calculating optical density (OD) values expressing the growth of these cells for 24 h at 37 °C and in three replicates for five concentrations (6.25), (12.5), (25), (50), and (100) µg/ml. MTT of cytotoxicity tests based on the results of average inhibition in percentages and as shown in Table No. (1), which proves that there is an inhibitory effect on the growth of cancer cells in B16 cell line starting from the concentration .256 µg/ml and the percentage of inhibition was 7% The percentage of inhibition for the second concentration increased by 12.5 µg/ml and reached 27%, and the

percentage of inhibition for the third concentration was 25 µg/ml was 44.67%, While the percentage of cell growth inhibition at the fourth concentration was 50 µg/ml 59%, while the highest percentage of inhibition of the cancer cells treated with ZnO-NPs was at the concentration 100 µg/ml and it was 78%. The line (Ref) did not have a significant effect on cell growth inhibition, as the percentage of inhibition ranged between 0.122 - 1.133%. In the above results of this study showed a very significant (statistically significant) cytostatic activity against tumor cells of the (B16) as line shown in Figure (4) and Table (1). The results indicate the ability of ZnO-NPs to inhibit the growth of B16 cancer cells using the IC50 concentration of 27.36 µg/ml, and that this effect depends on the concentration, the higher the concentration, greater the effect and this effect. Confirms that ZnO-NPs: safe and effective candidates for cancer cell growth limitation. Therefore, ZnO-NPs is expected to be considered as a new category of anticancer agents[8].

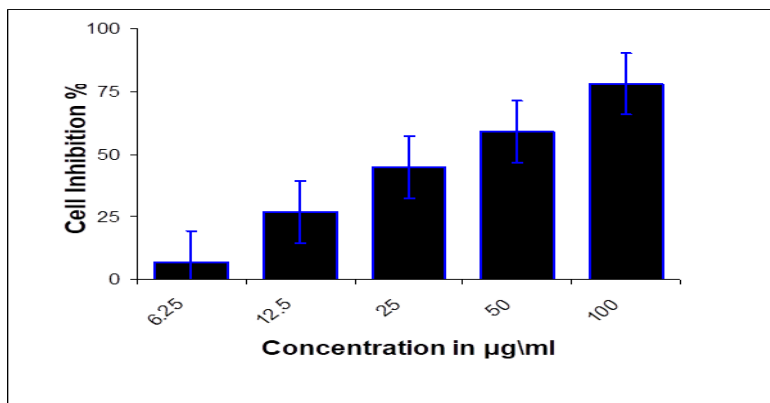


Figure 4 Toxic Effect of ZnO-NPs in Cells line (B16)

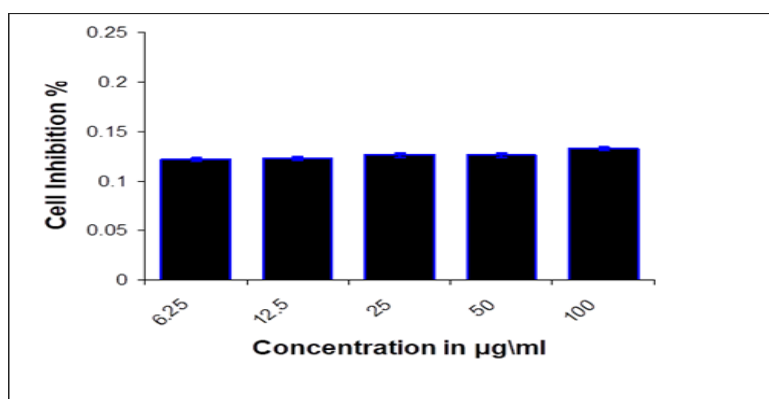


Figure 5 Toxic Effect of ZnO-NPs in Cells line (Ref)

Table(1) comparing toxicological effect of ZnO-NPs between cancer cells B16 and normal cells Ref

Concentration	B16 SE± M	Ref SE± M
6.25	2.08 ±7.000*	0.05 ± 1.10
12.5	2.30± 27.00*	0.11± 1.00
25	1.45±44.67*	0.02 ±0.65
50	2.30±59.00 *	0.01 ± 0.50
100	2.08±78.00*	0.05 ±0.40

The results showed the susceptibility of ZnO-NPs to causing (morphological) changes in the number, size and shape of B16 linear cancer cells for melanoma where the cells were monoclonal (monoclonal cells) as shown in Figure (6) before treatment With ZnO-NPs single cells became sparse in number and some became swollen and clearly affected by the exposed material, this is consistent with work done by Beiand coworkers in 2017 showing the ability of ZnO-NPs to cause significant cytotoxicity, leading to apoptosis in cells By increasing Reactive oxygen species (ROS) generation [17]. Numerous studies have shown the ability of different types of inorganic particles to inhibit the growth of cancer cells through several mechanisms such as free radicals and the ability of ions to release the mentioned particles in the association between different types of functional proteins are king inside the cell and thus hinder the work of proteins as a result of the change in Their nature and structure are three-dimensional, and these particles have the ability to penetrate the nucleus and bind to the genetic material and cause a dysfunction and thus cell death [18-19].

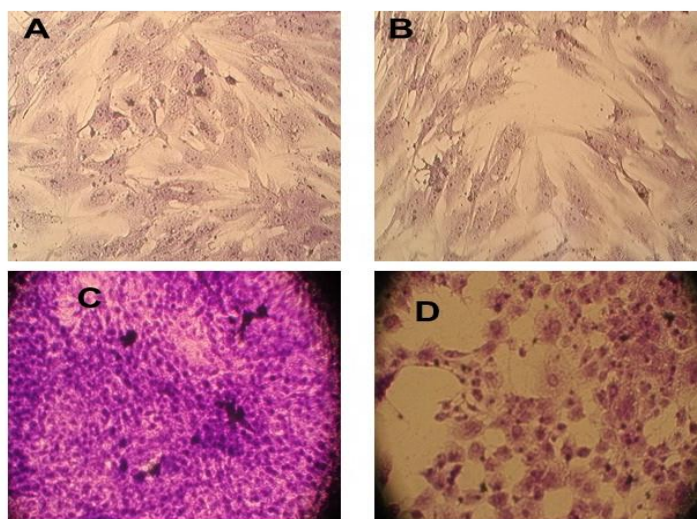


Figure (6): (A) Ref (Ctrl) (B) Ref -ZnO (2830 µg/ml) (C) Melanoma B16 (Ctrl) (D) Melanoma B16-ZnO (27.36 µg/ml)

Acknowledgments

We extend special thanks to all the staff at the Iraqi Center for Cancer and Medical Genetics Research for their assistance during data collection.

Ethical consent to share

The research was approved after the protocol was approved by Al-Mustansiriya University / Iraqi Center for Cancer and Medical Genetics Research (Reference: Official Book No. 897 issued on October 11, 2020).

References

1. Fitzmaurice, C., Allen, C., Barber, R. M., Barregard, L., Bhutta, Z. A., Brenner, H., & Satpathy, M. (2017). Global, regional, and national cancer incidence, mortality, years of life lost, years lived with disability, and disability-adjusted life-years for 32 cancer groups, 1990 to 2015: a systematic analysis for the global burden of disease study. *JAMA oncology*, 3(4), 524-548.
2. Paolino, G., Donati, M., Didona, D., Mercuri, S. R., & Cantisani, C. (2017). Histology of non-melanoma skin cancers: an update. *Biomedicines*, 5(4), 71.
3. Wang, K., Zhu, X., Yu, E., Desai, P., Wang, H., Zhang, C. L., ... & Hu, J. (2020). Therapeutic Nanomaterials for Neurological Diseases and Cancer Therapy. *Journal of Nanomaterials*.

4. Ziad T. Khodair, Mohanad W. Mahdi Alzubaidy, Asmaa M. SalihAlmohaidi, Ammar Ahmed Sultan, Sana M. H. AL-Shimmary, and Sarah S. Albusultan. Synthesis of copper oxide nanoparticles (CuO-NPs) and its evaluation of antibacterial activity against *P. aeruginosa* biofilm gene's. *Technologies and Materials for Renewable Energy, Environment and Sustainability AIP Conf. Proc.* 2190, 020006-1–020006-7; <https://doi.org/10.1063/1.5138492>, Published by AIP Publishing. 978-0-7354-1937-7/\$30.00
5. Zhang, Q., Li, H., Gan, L., Ma, Y., Golberg, D., &Zhai, T. (2016). In situ fabrication and investigation of nanostructures and nanodevices with a microscope. *Chemical Society Reviews*, 45(9), 2694-2713.
6. Akhter, M. H., Ahsan, M. J., Rahman, M., Anwar, S., &Rizwanullah, M. (2020). Advancement in nanotheranostics for effective skin cancertherapy: state of the art. *Current Nanomedicine (Formerly: Recent Patents on Nanomedicine)*, 10(2), 90-104.
7. Osman, D. A. M., & Mustafa, M. A. (2015). Synthesis and characterization of zinc oxide nanoparticles using zinc acetate dihydrate and sodium hydroxide. *Journal of Nanoscience and Nanoengineering*, 1(4), 248-251.
8. Wahab, Rizwan; Dwivedi, Sourabh; Umar, Ahmad; Singh, Surya; Hwang, I. H.; Shin, Hyung-Shik; Musarrat, Javed; Al-Khedhairy, Abdulaziz A.; Kim, Young-Soon (2013). ZnO Nanoparticles Induce Oxidative Stress in Cloudman S91 Melanoma Cancer Cells. *Journal of Biomedical Nanotechnology*, 9(3), 441–449. doi:10.1166/jbn.2013.1593.
9. Z. T. Khodair, A. A. Khadom, and H. A. Jasim, (2019) "Corrosion protection of mild steel in different aqueous media via epoxy/nanomaterial coating: preparation, characterization and mathematical views," *Journal of Materials Research and Technology*, vol.8, no.1, Pp.424-435, doi.org/10.1016/j.jmrt.2018.03.003.
10. Bouslimani, A., Porto, C., Rath, C. M., Wang, M., Guo, Y., Gonzalez, A., ... &Dorresteijn, P. C. (2015). Molecular cartography of the human skin surface in 3D. *Proceedings of the National Academy of Sciences*, 112(17), E2120-E2129.
11. Zotta, M. D., Nevins, M. C., Hailstone, R. K., &Lifshin, E. (2018). The determination and application of the point spread function in the scanning electron microscope. *Microscopy and Microanalysis*, 24(4), 396-405.
12. Jena, V. (2016). *Metastatic Cancer Chemistry*. Lulu. com.
13. Tolosa, L., Donato, M. T., & Gómez-Lechón, M. J. (2015). General cytotoxicity assessment by means of the MTT assay. In *Protocols in in vitro hepatocyte research* (pp. 333-348). Humana Press, New York, NY.
14. Feng, X., Yan, Y., Wan, B., Li, W., Jaisi, D. P., Zheng, L., ... & Liu, F. (2016). Enhanced dissolution and transformation of ZnO nanoparticles: the role of inositol hexakisphosphate. *Environmental science & technology*, 50(11), 5651-5660.
15. Kurugol, S., Kose, K., Park, B., Dy, J. G., Brooks, D. H., &Rajadhyaksha, M. (2015). Automated delineation of dermal–epidermal junction in reflectance confocal microscopy image stacks of human skin. *Journal of Investigative Dermatology*, 135(3), 710-717.
16. Jurablu, S., Farahmandjou, M., &Firoozabadi, T. P. (2015). Sol-gel of zinc oxide synthesis (ZnO) nanoparticles: study of structural and optical properties. *Journal of Sciences, Islamic Republic of Iran*, 26(3), 281-285.
17. Bai Ding-Ping, Xi-Feng Zhang, Guo-Liang Zhang, Yi-Fan Huang, SangiliyandiGurunathan. (2017). "Zinc oxide nanoparticles induce apoptosis and autophagy in human ovarian cancer cells," *International Journal of Nanomedicine*, vol. 12, pp. 6521–6535.
18. Bhattacharyya, S., Kudgus, R.A., Bhattacharya, R. and Mukherjee, P. (2011). *Inorganic Nanoparticles in Cancer Therapy*. *Pharm. Res.* 28:237–259
19. Probst, C. E., Zrazhevskiy, P., Bagalkot, V. and Gao, X. (2013). Quantum dots as a platform for nanoparticle drug delivery vehicle design. *Adv. Drug Delivery Rev.*65: 703–718.